High mobility solution-processed hybrid light emitting transistors

Bright Walker, Mujeeb Ullah, Gil Jo Chae, Paul L. Burn, Shinuk Cho, Jin Young Kim, Ebinazar B. Namdas, and Jung Hwa Seo

---

Articles you may be interested in

Comparing direct charge injection and Forster energy transfer into quantum dots in hybrid organic/inorganic quantum dot light emitting devices
J. Appl. Phys. **112**, 034501 (2012); 10.1063/1.4740234

Highly simplified small molecular phosphorescent organic light emitting devices with a solution-processed single layer
AIP Advances **1**, 032130 (2011); 10.1063/1.3625549

A gate dielectric that enables high ambipolar mobilities in polymer light-emitting field-effect transistors
Appl. Phys. Lett. **93**, 023301 (2008); 10.1063/1.2957472

High performance light emitting transistors
Appl. Phys. Lett. **92**, 183304 (2008); 10.1063/1.2920436

High-efficiency polymer light-emitting devices using organic salts: A multilayer structure to improve light-emitting electrochemical cells
Appl. Phys. Lett. **81**, 214 (2002); 10.1063/1.1490635

High mobility solution-processed hybrid light emitting transistors

Bright Walker,[1,a)] Mujeeb Ullah,[2,a)] Gil Jo Chae,[3,4] Paul L. Burn,[2] Shinuk Cho,[4] Jin Young Kim,[1] Ebinazar B. Namdas,[2,b)] and Jung Hwa Seo[3,b)]

[1]*School of Energy and Chemical Engineering, Ulsan National Institute of Science and Technology, Ulsan 689-798, South Korea*
[2]*Centre for Organic Photonics & Electronics, University of Queensland, Brisbane, Queensland 4072, Australia*
[3]*Department of Materials Physics, Dong-A University, Busan 604-714, South Korea*
[4]*Department of Physics and EHSRC, University of Ulsan, Ulsan 680-749, South Korea*

We report the design, fabrication, and characterization of high-performance, solution-processed hybrid (inorganic-organic) light emitting transistors (HLETs). The devices employ a high-mobility, solution-processed cadmium sulfide layer as the switching and transport layer, with a conjugated polymer Super Yellow as an emissive material in non-planar source/drain transistor geometry. We demonstrate HLETs with electron mobilities of up to $19.5 \, cm^2/V \, s$, current on/off ratios of $>10^7$, and external quantum efficiency of $10^{-2}\%$ at $2100 \, cd/m^2$. These combined optical and electrical performance exceed those reported to date for HLETs. Furthermore, we provide full analysis of charge injection, charge transport, and recombination mechanism of the HLETs. The high brightness coupled with a high on/off ratio and low-cost solution processing makes this type of hybrid device attractive from a manufacturing perspective. © 2014 AIP Publishing LLC.
[http://dx.doi.org/10.1063/1.4900933]

Solution processable organic semiconductors are set to play an important role in future display and lighting technologies due to their ability to be fabricated by economical, solution-based processes such as ink jet printing.[1,2] For the production of color organic light emitting diode (OLED) displays, each color pixel requires a transistor in order to supply current and modulate the light emission.[3] In commercially produced OLED displays, a backplane of polycrystalline silicon-based transistor elements are currently employed for this purpose.[4] Although advances in silicon processing by excimer laser annealing (ELA) have streamlined the processing and cost-effectiveness of polycrystalline silicon transistor backplanes and compatibility with OLED fabrication, the processing of the silicon backplane is still significantly more energy intensive and complicated than the solution-deposition of organic OLED components. As such, the use of polycrystalline silicon backplane defeats the advantages of OLEDs processed from solution. Thus, the development and integration of low-cost switching semiconductors and backplane circuitry is currently needed in order to fully realize the advantages of solution-processed organic semiconductors in OLED displays.

Organic light emitting field effect transistors (LEFETs) are a relatively new technology which combine the light emitting function of OLEDs with the switching function of field effect transistors (FET) in one device,[5–7] offering the potential to simplify the fabrication of display devices. Bilayer LEFETs containing a p-type conjugated polymer to act as a transport channel and achieve switching and an emissive conjugated polymer layer have enabled the tuning of the position of light emission to be near the negatively charged drain contact of the device.[8] LEFETs have also been demonstrated using a combination of p-type and n-type transport materials in a bipolar structure.[9–11] Although these LEFETs have been demonstrated to function effectively, the mobilities and/or low on/off ratios of the organic charge transport materials fall far below those of contemporary polycrystalline silicon drivers, limiting the intensity of light emission and performance. More recently, hybrid light emitting transistors (HLETs), in which metal oxides have been used as the charge transport layer, have led to devices that operate in n-type mode with higher mobilities and currents.[12]

Despite the interesting demonstration of the LEFET concept, to date, the absolute amount of light emitted from LEFETs has generally been low compared to OLED devices. While the mobility of polycrystalline silicon used in commercial OLED display back panels is on the order of $100–150 \, cm^2/V \, s$, the mobilities of LEFETs based on organic transport materials tend to be less than $\sim 1 \, cm^2/V \, s$. In the case of the solution processed metal oxide transport layers[12] the mobilities have been at best $\sim 5 \, cm^2/V \, s$; and for sputtered metal oxide transport layer[13] the mobilities have reached around $14 \, cm^2/V \, s$. These mobilities lead to smaller currents through the LEFETs compared to OLEDs on silicon backplanes, which makes it difficult to achieve bright light emission from the emissive layer.

In this contribution, we report HLET devices that make use of a high-electron-mobility, solution-processed CdS layer[14] to accomplish charge carrier transport and achieve high brightness from an emissive conjugated polymer layer. The measured mobilities of the n-type transport channel in the completed device are up to $19.5 \, cm^2/V \, s$ with current ON/OFF ratios of $>10^7$ in this configuration, allowing relatively high currents to pass through the emissive layer, yielding brightnesses of up to $2100 \, cd/m^2$.

a)B. Walker and M. Ullah contributed equally to this work.
b)Authors to whom correspondence should be addressed. Electronic addresses: e.namdas@uq.edu.au and seojh@dau.ac.kr.
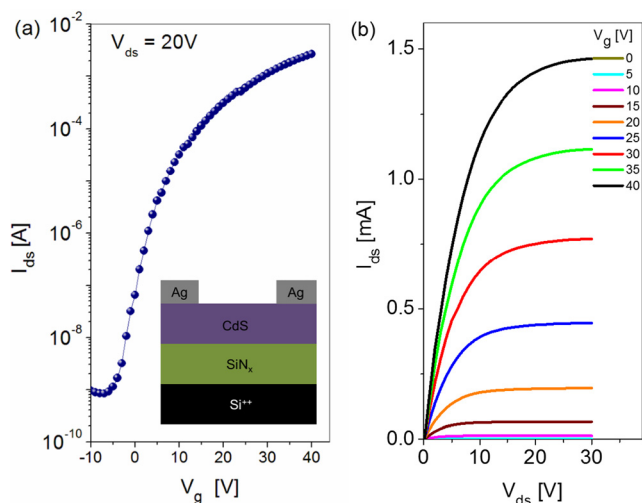
FIG. 1. (a) Transfer characteristics of the control CdS FET, device structure given in inset. (b) Output characteristics of the CdS FET. The channel width and length of the FETs were 3 mm and 50 μm, respectively.

The CdS layer used in this work was formed in the following manner. Cadmium tert-nonanethiolate[14] was dissolved in chloroform in a nitrogen filled glovebox at a concentration of 6 mg/ml. The solution was passed through a 0.45 μm PTFE syringe filter (with some difficulty) and kept in a pre-cleaned vial. The solution was spin-coated by rapidly dispensing 40 μl at a time (using a micropipette) onto pre-cleaned Si/SiN$_x$ substrates (SiN$_x$ thickness = 450 nm) which were already spinning at 1500 rpm. The films were then annealed on a hotplate under a nitrogen atmosphere at 300 °C for 5 min. A second layer of CdS was deposited in the same manner and annealed at 300 °C for 30 min. Thin film transistors from CdS layers were fabricated using Ag as source and drain electrodes as shown in Fig. 1(a) inset. The electrical transfer and output characteristics of the simple CdS FETs are shown in Figs. 1(a) and 1(b), respectively. From transfer characteristics an average electron mobility of 21 ± 3 cm^2/V s was calculated in the saturation regime, with on/off ratios of up to 5 × 10^6 indicating excellent switching properties of the devices.

Fig. 2 shows the HLET architecture, structure of the commercially available lightemitting paraphenylenevinylene based polymer Super Yellow (SY), and charge injection mechanism of the HLETs. Two shadow masks were used in combination during the thermal evaporation of the source and drain electrodes in order to form interdigitated hole-injecting

and electron-injecting non-planar contacts. The electron-injecting contact was deposited directly on the top of the CdS layer by evaporating 50 nm of Ag. SY was purchased from Merck (PDY–132) and used without further purification. SY films were spin-coated on top of the CdS layer from a 7 mg/ml toluene (>99.9%, anhydrous) solution at 2500 rpm for 45 s, then at 3000 rpm for 15 s to ensure the films were dry. The substrates were then baked on a hot plate at 150 °C for 10 min. A ~15 nm MoO$_x$ layer was evaporated onto the SY film followed by a 50 nm Au layer to form the hole-injecting contact. The thickness of each layer was measured using a quartz crystal monitor during evaporation and verified using a Dektak 150 profilometer. The channel width and lengths of the HLETs were 16 mm and 70 μm, respectively. The performance of at least 5 devices was used to calculate average device parameters. Errors were calculated using the standard deviation of the results. The electrical and optical characteristics of the devices were tested using an Agilent B1500A Semiconductor Device Analyzer and an SA-6 Semi-Auto Prober with a calibrated photomultiplier tube (pmt) positioned over the device. All the device fabrication and testing were performed inside a nitrogen filled MBraun glove box (O$_2$ and H$_2$O levels <0.1 ppm). The characterization set up details have been reported previously.[10–12] In Fig. 2(c), the highest occupied molecular orbital (HOMO) of the SY was measured using photoelectron spectroscopy in air (PESA). In order to estimate the lowest unoccupied molecular orbital (LUMO), the optical gap was determined from solid-state measurements and added to the ionization potential. The optical gap was determined from the intersection of the normalized absorption and photoluminescence spectra plotted in energy. The conduction and valence bands of the CdS were determined by ultraviolet photoelectron spectroscopy (UPS).[14]

Fig. 3(a) shows the output and transfer characteristics (black circles) of the hybrid CdS/SY HLET device. Typical n-type transistor behavior was observed for this device structure, as shown by the drain current (I_{ds}) versus source drain voltage (V_{ds}) curves at various positive gate voltages (V_g) in Fig. 3. No light emission was observed from CdS transistors without the SY layer, while emission of light corresponding to the SY layer was observed with hybrid CdS/SY devices. These observations imply that the CdS and SY function as an electron transport material and an emissive material, respectively. No evidence of hole transport across the channel under negative bias was observed. Analysis of the curves in Fig. 3(b) yields an average electron mobility (μ) of
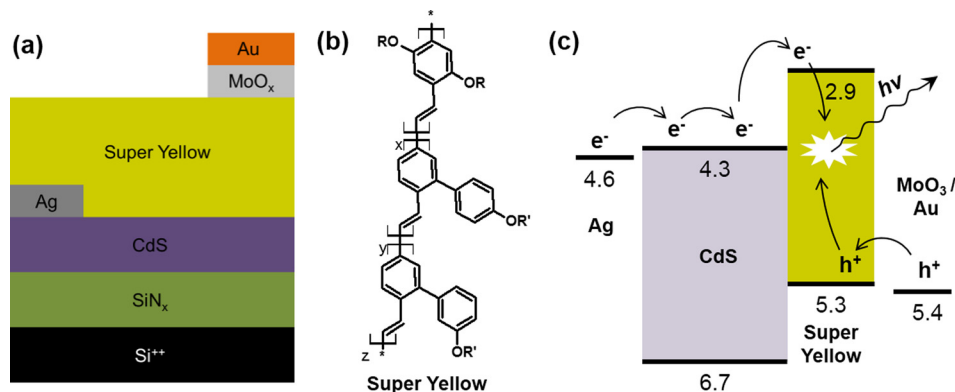

FIG. 2. (a) HLET device structure, (b) chemical structure of SY, and (c) energy levels of materials used in this work.
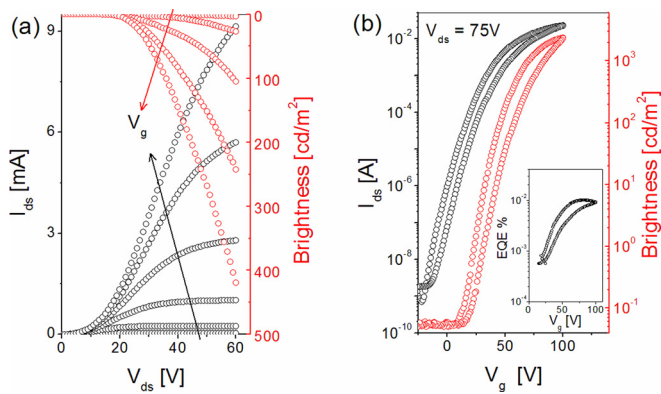
FIG. 3. (a) Electrical output (black circles) and optical output (red circles) characteristics of the HLET configuration $Si/SiN_x/Ag/CdS/SY/MoO_x/Au$. ($V_g$ was scanned from 0 to 60 V at intervals of 10 V). (b) Electrical transfer (black circles) and optical transfer (red circles) characteristics (V_{ds} fixed at 75 V) of the corresponding device in (a). External quantum efficiency of HLETs as a function of V_g is given as an inset.

13.4 cm^2/V s, while the highest value was observed to be 19.5 ± 0.5 cm^2/V s, with an on/off ratio of $\sim 5 \times 10^7$. We here report the highest electron mobility observed to date in solution based LEFETs or HLETs.

Fig. 3(b) show the optical output (red circle) versus V_{ds} at various V_g and the optical transfer characteristics versus V_g at $V_{ds} = 75$ V. As shown by the brightness (cd/m^2) versus V_{ds} plots, the brightness increases with V_{ds} and V_g. The light emission zone was stationary and occurred primarily under the hole injecting MoO_x/Au electrode, which is characteristic of an unipolar HLET. A magnified optical image of the working device is shown in Fig. 4. The HLET exhibited an average brightness of 1983 ± 100 cd/m^2, with a peak brightness of 2100 cd/m^2, and an efficiency of 10^{-2}%. We note that the MoO_x/Au electrode was not transparent and thus the measurable light was that which escaped around the edges of the electrode, leading to a lower external quantum efficiency (EQE) than might have been expected. The width of the observable emission zone was estimated from the micrographs to be $30 \pm 5 \mu m$. Nevertheless, in spite of this
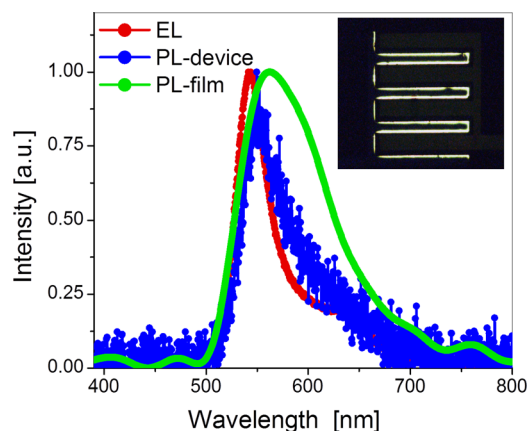

FIG. 4. PL and EL spectra of the hybrid CdS/SY HLET: EL spectra of the device (red curve); the blue curve is PL from the device, i.e., $Si-wafer/SiN_x/CdS/SY/MoO_x/Au$; and the green curve is PL of SY film on a quartz substrate. Inset shows an optical photograph of an operating yellow-green HLET. The light emission zone was primarily under the hole-injecting electrode.

these combined EQE and brightness exceed those reported to date for hybrid light emitting transistors.[12,13] Taking these observations into account, the mechanism for operation of these hybrid LEFETs involves injection of electrons from the Ag source electrode into the conduction band of the CdS (4.3 eV),[14] transport of electrons along the CdS/dielectric interface, injection of electrons from the conduction band of CdS into the LUMO of SY (2.9 eV) where they subsequently recombine with holes injected from the MoO_x/Au drain electrode into the HOMO of SY (5.3 eV; measured by PESA).[12] Under these circumstances, carrier recombination occurs within the SY layer near the positively biased drain electrode, leading to light emission as illustrated in Fig. 2(c). We note that the non-planar source-drain device geometry is critical for light emission. Because it reduces the contact resistance for the electrons[12] and forces the carriers to pass through the emissive layer leading to radiative recombination. We envision that the efficiency of these devices could be further improved via the incorporation of an electron injection layer to overcome the large electron injection barrier between the conduction band of CdS (4.3 eV) and the LUMO of SY (2.9 eV).[12]

A typical electroluminescence (EL) spectrum for the hybrid LEFET is displayed in Fig. 4. Also shown is the corresponding photoluminescence (PL) spectrum for of the device, and PL spectra of the SY/quartz film. The EL spectrum is similar to the PL spectra of the device; it is noteworthy that both the EL and PL of the SY film in the device architecture show slightly narrower and blue-shifted spectra compared to the PL spectrum of SY deposited on a quartz substrate, consistent with a micro cavity effect in the device configuration. Given that the optical gap of the CdS layer is similar to the SY layer, the possibility that light emission from the CdS layer contributes to the change in emission spectrum must be considered. However, as stated earlier the CdS FETs without a SY layer did not exhibit EL and the CdS layer alone was not fluorescent. In our device, a weak micro-cavity could be formed by the MoO_x/Au mirror and refractive index mismatch between the various organic and inorganic layers in the cavity. Furthermore, the silicon wafer is a good reflector due to its high refractive index ($n \sim 3.6$).[15]

In summary, hybrid LEFETs were demonstrated using a solution processed CdS layer in conjunction with a light emitting conjugated polymer. The device with fully solution processed active layers exhibits an outstanding on/off ratio of up to 10^8 and a large electron mobility of up to 19.5 cm^2/V s, allowing significant currents to pass through the emissive layer and produce a brightness of up to 2100 cd/m^2. The performance of this device architecture approaches, within an order of magnitude, the performance of commercial ELA polycrystalline silicon transistor backplane elements.

[1]T. W. Kelley, P. F. Baude, C. Gerlach, D. E. Ender, D. Muyres, M. A. Haase, D. E. Vogel, and S. D. Theiss, Chem. Mater. **16**, 4413 (2004).

[2]J.-S. Park, H. Chae, H. K. Chung, and S. I. Lee, Semicond. Sci. Technol. **26**, 034001 (2011).

[3]T. Tsujimura, *OLED Displays* (John Wiley & Sons, Inc., 2012), pp. 69–103.

[4]J. Wang, L. Sun, D. Han, Y. Wang, M. Chan, and S. Zhang, J. Disp. Technol. **10**, 317 (2014).

[5]A. Hepp, H. Heil, W. Weise, M. Ahles, R. Schmechel, and H. Von Seggern, Phys. Rev. Lett. **91**, 157406 (2003).

[6]M. Muccini, Nat. Mater. **5**, 605 (2006).

[7]J. Zaumseil, R. H. Friend, and H. Sirringhaus, Nat. Mater. **5**, 69 (2006).

[8]E. B. Namdas, P. Ledochowitsch, J. D. Yuen, D. Moses, and A. J. Heeger, Appl. Phys. Lett. **92**, 183304 (2008).

[9]R. Capelli, S. Toffanin, G. Generali, H. Usta, A. Facchetti, and M. Muccini, Nat. Mater. **9**, 496 (2010).

[10]M. Ullah, K. Tandy, S. D. Yambem, M. Aljada, P. L. Burn, P. Meredith, and E. B. Namdas, Adv. Mater. **25**, 6213 (2013).

[11]K. Tandy, M. Ullah, P. L. Burn, P. Meredith, and E. B. Namdas, Org. Electron. **14**, 2953 (2013).

[12]K. Muhieddine, M. Ullah, B. N. Pal, P. Burn, and E. B. Namdas, Adv. Mater. **26**, 6410 (2014).

[13]H. Nakanotani, M. Yahiro, C. Adachi, and K. Yano, Appl. Phys. Lett. **90**, 262104 (2007).

[14]B. Walker, G.-H. Kim, J. Heo, G. J. Chae, J. Park, J. H. Seo, and J. Y. Kim, RSC Adv. **4**, 3153 (2014).

[15]H. H. Li, J. Phys. Chem. Ref. Data **9**, 561 (1980).